General Expressions for IM/DD Dispersive Analog Optical Links With External Modulation or Optical Up-Conversion in a Mach–Zehnder Electrooptical Modulator

Juan L. Corral, *Member, IEEE*, Javier Marti, *Member, IEEE*, and Jose M. Fuster

***Abstract*—A general derivation of the optical modulation process in a dual-drive Mach–Zehnder modulator (DD-MZM) is introduced. The expressions include all harmonics and are entirely general in terms of bias point. Chromatic dispersion is also included allowing the prediction of a number of important phenomena in photonic signal transmission. Examples of special cases of these general equations are then presented. Similar expressions are introduced for harmonic optical up-conversion through a photonic mixer based on a DD-MZM covering any bias point or phase shift between DD-MZM drives.**

***Index Terms*—Electrooptic modulation, Mach–Zehnder electrooptical modulator, nonlinear distortion, optical communication, optical fiber dispersion, optical frequency conversion, optical modulation/demodulation, optical propagation in dispersive media.**

I. Introduction

THE Mach–Zehnder electrooptical modulator (MZM) has been thoroughly used for the generation and transmission of microwave/millimeter-wave signals [1], [2]. In the conventional case, the MZM is biased at its most linear point [also known as quadrature bias (QB)] and driven directly by the microwave signal in such a way that a double-sideband plus carrier (DSB $+$ C) modulation is obtained. The performance of this modulation is severely limited by the chromatic dispersion of the optical link [3], which is the most relevant impairment in optical microwave/millimeter-wave transmission systems operating near 1550 nm. Chromatic dispersion also limits the performance of dispersive optical devices like the tunable delay lines based on highly dispersive fiber or chirped fiber gratings [4], [5]. In order to mitigate this limitation, an optical single-sideband plus carrier (SSB $+$ C) modulation was proposed by using a dual-drive Mach–Zehnder modulator (DD-MZM) [5], [6].

Optical harmonic up-converting techniques have been proposed and demonstrated employing either a standard MZM biased at the nonlinear operating region (minimum (MITB) or maximum (MATB) transmission bias point) [2], [7]–[9] or DD-MZM biased to behave like a harmonic single side-band (HSSB) optical up-converter [10].

All these modulation or up-conversion schemes are based on biasing the DD-MZM (standard MZM is a particular case of the DD-MZM modulator) on different points (QB, MATB, and MITB) and introducing a phase shift ($0, \pi/2$, or π) between both electrodes signals. Previous studies in the literature are limited to first-order approximations of all these different cases. In this paper, the optical modulation process in a DD-MZM modulator is analyzed in a simple and rigorous way including the effect of the optical link dispersion.

This paper is organized as follows. In Section II, the general expression for the use of a DD-MZM as an electrooptical modulator in an IM/DD dispersive link are obtained, while Section III is devoted to extracting the general expression when the DD-MZM is used as an electrooptical up-converter. Section IV collects the particular expressions and main results for five different modulation or up-conversion schemes (DSB $+$ C, SSB $+$ C, HSSB, MITB, MATB) making references to the general expressions introduced in Sections II and III. Finally, the validity of these expressions is assessed in Section V and some conclusions are presented in Section VI.

II. Case 1: DD-MZM as a Modulator

The electrical voltages applied on both electrodes of a DD-MZM modulator (Fig. 1) will be composed of a dc term and an RF component (same amplitude but arbitrary phases)

$$\begin{aligned} V_1(t) &= V_{\mathrm{DC1}} + v_{\mathrm{RF}} \sin(\omega_{\mathrm{RF}} t + \phi_{\mathrm{RF1}}) \\ V_2(t) &= V_{\mathrm{DC2}} + v_{\mathrm{RF}} \sin(\omega_{\mathrm{RF}} t + \phi_{\mathrm{RF2}}). \end{aligned} \tag{1}$$

It is important to point out that, according to (1) and Fig. 1, a standard MZM is a particular case of the DD-MZM modulator where $\phi_{\mathrm{RF1}} = \phi_{\mathrm{RF2}} \pm \pi$. If the MZM is driven according to the voltages from (1) and the optical field with optical frequency ω_c at the MZM input is

$$E_{\mathrm{input}} = \sqrt{2P} e^{j\phi_o} \tag{2}$$

where P is the optical power, then the optical field at the MZM

Manuscript received January 5, 2001; revised May 26, 2001. This work was supported by the Spanish Research and Technology Commission (CICYT) for funding the Project TIC2000-1674 and the European Commission for funding the Project IST-2000-25390 (OBANET).

The authors are with ETSI Telecomunicacion, Universitat Politecnica de Valencia, 46022 Valencia, Spain (e-mail: jlcorral@ieee.org).

Publisher Item Identifier S 0018-9480(01)08719-1.

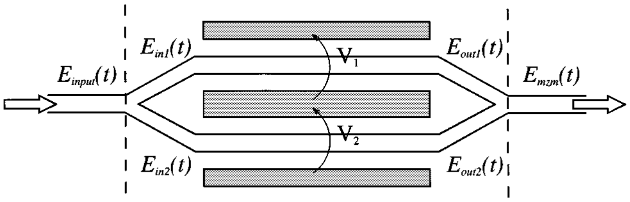

Fig. 1. Dual-drive Mach–Zehnder (DD-MZM) electrooptical modulator.

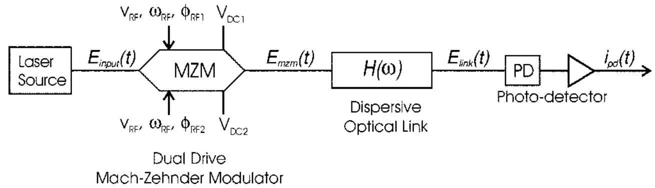

Fig. 2. Externally modulated (DD-MZM) analog dispersive optical link.

output is

$$E_{\mathrm{mzm}}(t) = \sqrt{2Pt_{ff}}e^{j\phi_c} \sum_{n=-\infty}^{\infty} J_n(m_{\mathrm{RF}}) \cdot \cos(\phi_v + n\phi_d) e^{jn(\omega_{\mathrm{RF}}t + \phi_m)} \quad (3)$$

where $J_n(x)$ is the Bessel function of first kind and order n, t_{ff} are the MZM insertion losses, and

$$m_{\mathrm{RF}} = \frac{\pi v_{\mathrm{RF}}}{V_\pi} \quad (4a)$$

$$\phi_c = \phi_e + \frac{\pi(V_{\mathrm{DC1}} + V_{\mathrm{DC2}})}{2V_\pi} \quad (4b)$$

$$\phi_m = \frac{\phi_{\mathrm{RF1}} + \phi_{\mathrm{RF2}}}{2} \quad (4c)$$

$$\phi_v = \frac{\pi(V_{DC1} - V_{\mathrm{DC2}})}{2V_\pi} \quad (4d)$$

$$\phi_d = \frac{\phi_{\mathrm{RF1}} - \phi_{\mathrm{RF2}}}{2} \quad (4e)$$

where V_π is the MZM switching voltage and $\phi_e - \phi_o$ is the optical insertion phase at $\omega = \omega_c$ when no voltages are applied at the drives.

In Fig. 2, an analog IM/DD optical link with a DD-MZM used as an electrooptical modulator is sketched. The dispersive link is modeled with a frequency response as

$$H_{\mathrm{link}}(\omega) = |H_{\mathrm{link}}(\omega)| \, e^{j\theta_{\mathrm{link}}(\omega)} \quad (5)$$

where ω is the frequency of the optical signal. The frequency response of the dispersive link is assumed to be flat in amplitude and parabolic in phase inside the optical signal bandwidth around optical carrier frequency $\omega = \omega_c$

$$\begin{cases} |H_{\mathrm{link}}(\omega)| = \dfrac{1}{\sqrt{L}} \\ \theta_{\mathrm{link}}(\omega) = \theta_o + \theta_1(\omega - \omega_c) + \dfrac{\theta_2}{2}(\omega - \omega_c)^2 \end{cases} \quad (6)$$

where L is the optical power loss of the dispersive link, θ_0 and θ_1 are the insertion phase and group time delay of the dispersive link at $\omega = \omega_c$, respectively, and θ_2 is the first-order dispersion term.

As the optical signal at the MZM output from (3) passes through an optical dispersive link with a frequency response defined by (6), the optical signal at the link output is

$$E_{\mathrm{link}}(t) = \sqrt{\frac{2Pt_{ff}}{L}} \, e^{j\phi_{\mathrm{link}}} \sum_{n=-\infty}^{\infty} J_n(m_{\mathrm{RF}}) C_{\mathrm{DC}}(n) \cdot e^{j(n\omega_{\mathrm{RF}}(t+\theta_1) + n\phi_m + (\theta_2/2)\, n^2 \omega_{\mathrm{RF}}^2)} \quad (7)$$

where $C_{\mathrm{DC}}(n) = \cos(\phi_v + n\phi_d)$ and $\phi_{\mathrm{link}} = \phi_c + \theta_o$.

Furthermore, as this optical signal is detected by an ideal photodetector with responsivity $\Re$, the temporal expression of the detected current can be calculated from the envelope of the incident optical signal and expressed as (8), shown at the bottom of this page, where

$$I(n) = J_n(m_{\mathrm{RF}}) C_{\mathrm{DC}}(n). \quad (9)$$

Finally, by simple manipulation in (8), we have

$$i_{\mathrm{pd}}(t) = \frac{\Re P t_{ff}}{L} \left(I_{\mathrm{DC}} + \sum_{p=1}^{\infty} I_{p\mathrm{RF}}(p) \right) \quad (10)$$

where

$$I_{\mathrm{DC}} = \sum_{n=-\infty}^{\infty} I^2(n) = \sum_{n=-\infty}^{\infty} J_n^2(m_{\mathrm{RF}}) C_{\mathrm{DC}}^2(n) \quad (11a)$$

$$I_{p\mathrm{RF}}(p) = 2 \sum_{n=-\infty}^{\infty} I(n) I(n-p) \cdot \cos\left(p\omega_{\mathrm{RF}}(t+\theta_1) + p\phi_m + \frac{\theta_2}{2} p(2n-p)\omega_{\mathrm{RF}}^2 \right). \quad (11b)$$

Equations (10) and (11) show that the detected signal includes a dc term and harmonics of the modulating signal frequency. The dc term from (11a) depends on both the MZM biasing point and the optical modulation index rather than the optical link dispersion. The expression of the pth harmonic of the RF at the detected signal in (11b) is the sum of different beats of frequency components of the optical signal which are separated by $p\omega_{\mathrm{RF}}$.

$$i_{\mathrm{pd}}(t) = \frac{\Re E_{\mathrm{link}} E_{\mathrm{link}}^*}{2} = \frac{\Re P t_{ff}}{L} \sum_{p=-\infty}^{\infty} \left[\sum_{n=-\infty}^{\infty} I(n) I(n-p) e^{j(p\omega_{\mathrm{RF}}(t+\theta_1) + p\phi_m + (\theta_2/2)\, p(2n-p)\omega_{\mathrm{RF}}^2)} \right] \quad (8)$$

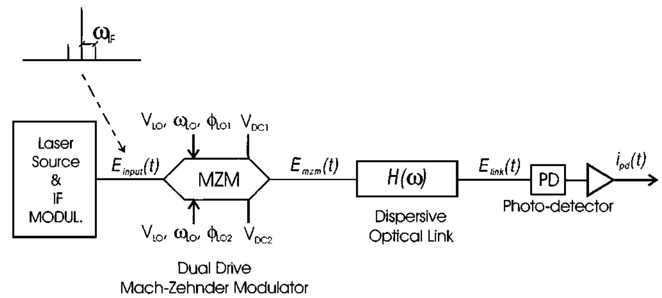

Fig. 3. Optical up-conversion of an IF modulated optical signal through a DD-MZM in an analog dispersive optical link.

III. Case 2: DD-MZM as an Up-Converter

The configuration of the IM/DD optical link using a DD-MZM as a harmonic up-converter is shown in Fig. 3, where a DD-MZM is placed at the transmitter side in order to up-convert an intermediate frequency (IF) signal which modulates the intensity of an optical carrier. If the IF modulation stage is assumed to be ideal, the optical field at the DD-MZM input is

$$E_{\rm IF}(t) = \sqrt{2P}\left(1+\frac{m_{\rm IF}}{2}\cos(\omega_{\rm IF}t+\phi_{\rm IF})\right)e^{j\phi_o} \tag{12}$$

where $m_{\rm IF}$ is the IF intensity modulation index. The optical field after the up-conversion stage at the MZM (assumed to be linear from the optical point of view) may be expressed as

$$E_{\rm mzm}(t) = \sqrt{2Pt_{ff}}e^{j\phi_c}\left(1+\frac{m_{\rm IF}}{2}\cos(\omega_{\rm IF}t+\phi_{\rm IFe})\right) \cdot \sum_{n=-\infty}^{\infty} J_n(m_{\rm LO})C_{\rm DC}(n)e^{j(n\omega_{\rm LO}t+n\phi_m)} \tag{13}$$

where $\phi_{\rm IFe}$ takes into account the difference between the MZM insertion phases for the three optical components at MZM input. The other parameters in (13) are defined as in (4), but $m_{\rm LO}$ corresponds to $m_{\rm RF}$ of (4a).

As the optical signal at the MZM output from (13) passes through an optical dispersive link with a frequency response defined as in (6), the optical signal at the link output is (14), shown at the bottom of this page. After detection using an ideal photodetector with responsivity $\Re$, the temporal expression of the detected current may be expressed as

$$i_{\rm pd}(t) = \frac{\Re P t_{ff}}{L}\Bigg[I_{\rm DC}+I_{\rm IF}+I_{\rm 2IF} + \sum_{p=1}^{\infty}\Big[I_{p{\rm LO}}(p)+I_{p{\rm LO+IF}}(p)+I_{p{\rm LO-IF}}(p) + I_{p{\rm LO+2IF}}(p)+I_{p{\rm LO-2IF}}(p)\Big]\Bigg] \tag{15}$$

where $I(n)$ from (9) and the eight different terms in (15) correspond to

$$I_{\rm DC} = \left[1+\frac{m_{\rm IF}^2}{8}\right]\sum_{n=-\infty}^{\infty} I^2(n) = \left[1+\frac{m_{\rm IF}^2}{8}\right]\sum_{n=-\infty}^{\infty} J_n^2(m_{\rm LO})C_{\rm DC}^2(n) \tag{16a}$$

$$I_{\rm IF} = m_{\rm IF}\sum_{n=-\infty}^{\infty} I^2(n)\cos\left(\frac{\theta_2}{2}\,\omega_{\rm IF}^2\right) \cdot\cos\left(\omega_{\rm IF}(t+\theta_1)+\phi_{\rm IFe}+\theta_2 n\omega_{\rm LO}\omega_{\rm IF}\right) \tag{16b}$$

$$I_{\rm 2IF} = \frac{m_{\rm IF}^2}{8}\sum_{n=-\infty}^{\infty} I^2(n) \cdot\cos\left(2\omega_{\rm IF}(t+\theta_1)+2\phi_{\rm IFe}+\theta_2 n\omega_{\rm LO}2\omega_{\rm IF}\right) \tag{16c}$$

$$I_{p{\rm LO}}(p) = 2\left[1+\frac{m_{\rm IF}^2}{8}\cos(\theta_2 p\omega_{\rm LO}\omega_{\rm IF})\right] \cdot\sum_{n=-\infty}^{\infty} I(n)I(n-p) \cdot\cos\left(p\omega_{\rm LO}(t+\theta_1)+p\phi_m+\frac{\theta_2}{2}\,p(2n-p)\omega_{\rm LO}^2\right) \tag{16d}$$

$$I_{p{\rm LO+IF}}(p) = m_{\rm IF}\cos\left(\frac{\theta_2}{2}\,\omega_{\rm IF}(p\omega_{\rm LO}+\omega_{\rm IF})\right) \cdot\sum_{n=-\infty}^{\infty} I(n)I(n-p) \cdot\cos\Big((p\omega_{\rm LO}+\omega_{\rm IF})(t+\theta_1)+p\phi_m+\phi_{\rm IFe} + \frac{\theta_2}{2}(2n-p)\omega_{\rm LO}(p\omega_{\rm LO}+\omega_{\rm IF})\Big) \tag{16e}$$

$$I_{p{\rm LO-IF}}(p) = m_{\rm IF}\cos\left(\frac{\theta_2}{2}\,\omega_{\rm IF}(p\omega_{\rm LO}-\omega_{\rm IF})\right) \cdot\sum_{n=-\infty}^{\infty} I(n)I(n-p) \cdot\cos\Big((p\omega_{\rm LO}-\omega_{\rm IF})(t+\theta_1)+p\phi_m-\phi_{\rm IFe} + \frac{\theta_2}{2}(2n-p)\omega_{LO}(p\omega_{\rm LO}-\omega_{\rm IF})\Big) \tag{16f}$$

$$E_{\rm link}(t) = \sqrt{\frac{2Pt_{ff}}{L}}\,e^{j\phi_{\rm link}}\left[\sum_{n=-\infty}^{\infty}\Big[J_n(m_{\rm RF})C_{\rm DC}(n)\;e^{j(n\omega_{\rm LO}(t+\theta_1)+n\phi_m+(\theta_2/2)\,n^2\omega_{\rm LO}^2)} \cdot\left(1+\frac{m_{\rm IF}}{2}\,e^{j(\theta_2/2)\,\omega_{\rm IF}^2}\;\cos\left(\omega_{\rm IF}(t+\theta_1)+\phi_{\rm IFe}+\theta_2 n\omega_{\rm LO}\omega_{\rm IF}\right)\right)\Big]\right] \tag{14}$$

$$I_{\mathrm{pLO+2IF}}(p) = \frac{m_{\mathrm{IF}}^2}{8} \sum_{n=-\infty}^{\infty} I(n)I(n-p) \cdot \cos\left((p\omega_{\mathrm{LO}}+2\omega_{\mathrm{IF}})(t+\theta_1)+p\phi_m+2\phi_{\mathrm{IFe}} + \frac{\theta_2}{2}(2n-p)\omega_{\mathrm{LO}}(p\omega_{\mathrm{LO}}+2\omega_{\mathrm{IF}})\right) \tag{16g}$$

$$I_{\mathrm{pLO-2IF}}(p) = \frac{m_{\mathrm{IF}}^2}{8} \sum_{n=-\infty}^{\infty} I(n)I(n-p) \cdot \cos\left((p\omega_{\mathrm{LO}}-2\omega_{\mathrm{IF}})(t+\theta_1)+p\phi_m-2\phi_{\mathrm{IFe}} + \frac{\theta_2}{2}(2n-p)\omega_{\mathrm{LO}}(p\omega_{\mathrm{LO}}-2\omega_{\mathrm{IF}})\right). \tag{16h}$$

Detected current includes three terms (I_{DC}, I_{IF}, I_{2IF}) around dc and five terms (I_{pLO}, $I_{p\mathrm{LO}\pm\mathrm{IF}}$, $I_{p\mathrm{LO}\pm 2\mathrm{IF}}$) around each harmonic of the LO signal inserted into the DD-MZM up-converter. Depending on the particular DD-MZM driving conditions, some of these terms may vanish.

IV. Particularized Expressions

A. Double-Sideband Plus Carrier Modulation (DSB + C)

For conventional intensity modulation (DSB + C), the DD-MZM is biased at the linear point, $|V_{DC1}-V_{DC2}| = V_\pi/2$, with a phase shift between electrodes of $|\phi_{RF1}-\phi_{RF2}| = \pi$.

In this case, the different components of the detected signal from (11) may be simplified as

$$I_{\mathrm{DC}} = \sum_{n=-\infty}^{\infty} I^2(n) = \sum_{n=-\infty}^{\infty} J_n^2(m_{\mathrm{RF}})\cos^2\left(\frac{\pi}{4} \pm n\frac{\pi}{2}\right) = \frac{1}{2}\sum_{n=-\infty}^{\infty} J_n^2(m_{RF}) = \frac{1}{2} \tag{17a}$$

$$I_{p\mathrm{RF}}(p) = \cos(p\omega_{\mathrm{RF}}(t+\theta_1)+p\phi_m) \cdot \left[J_{p/2}^2(m_{\mathrm{RF}}) + 2(-1)^{p/2}\sum_{n=(p/2)+1}^{\infty} J_n(m_{\mathrm{RF}}) \cdot J_{n-p}(m_{\mathrm{RF}})\cos\left(\frac{\theta_2}{2}p(2n-p)\omega_{\mathrm{RF}}^2\right)\right] \tag{17b}$$

for even harmonics of RF signal (p even) and

$$I_{p\mathrm{RF}}(p) = \pm 2\cos(p\omega_{\mathrm{RF}}(t+\theta_1)+p\phi_m) \cdot \sum_{n=(p+1)/2}^{\infty} (-1)^{n-(p-1)/2} J_n(m_{\mathrm{RF}})J_{n-p}(m_{\mathrm{RF}}) \cdot \cos\left(\frac{\theta_2}{2}p(2n-p)\omega_{RF}^2\right) \tag{17c}$$

for fundamental and odd harmonics of RF signal (p odd). The sign ambiguity in (17c) comes from the selection of the bias point and it will have no influence on the relative level of the harmonics.

As expected, the dc term is independent of m_{RF} or link dispersion (characterized by θ_2), but the level of the different harmonics of the modulating signal are clearly dependent on both terms.

As an example of the results that may be obtained from (17a)–(17c), the level of the RF component of the detected signal against phase dispersion term $\theta_d = (\theta_2\omega_{\mathrm{RF}}^2)/2$ (a term which is directly proportional to the total optical link dispersion and proportional to the square of the signal frequency, so both responses against total dispersion (proportional to optical link length) or frequency can be estimated) is shown in Fig. 4 (for five different values of optical modulation index m_{RF}).

B. Single-Sideband Plus Carrier Modulation (SSB + C)

To generate an optical single-sideband modulation, the DD-MZM has to be biased at the linear point, $|V_{\mathrm{DC1}} - V_{\mathrm{DC2}}| = V_\pi/2$, with a phase shift between MZM drives of $|\phi_{\mathrm{RF1}}-\phi_{\mathrm{RF2}}| = \pi/2$. In this case, the different components of the detected signal (dc term and harmonics of the RF frequency) from (11) would reduce to

$$I_{\mathrm{DC}} = \sum_{n=-\infty}^{\infty} I^2(n) = \sum_{n=-\infty}^{\infty} J_n^2(m_{\mathrm{RF}})\cos^2\left(\frac{\pi}{4} \pm n\frac{\pi}{2}\right) = \frac{J_0^2(m_{\mathrm{RF}})}{2} + \sum_{n=1}^{\infty} J_n^2(m_{\mathrm{RF}}) = \frac{1}{2} \tag{18a}$$

$$I_{p\mathrm{RF}}(p) = \cos\left(p\frac{\pi}{4}\right)\cos(p\omega_{\mathrm{RF}}(t+\theta_1)+p\phi_m) \cdot \left[J_{p/2}^2(m_{\mathrm{RF}})(-1)^{p/2} + 2\sum_{n=p/2+1}^{\infty} J_n(m_{\mathrm{RF}}) \cdot J_{n-p}(m_{\mathrm{RF}})\cos\left(\frac{\theta_2}{2}p(2n-p)\omega_{\mathrm{RF}}^2\right)\right] \mp 2\sin(p\omega_{\mathrm{RF}}(t+\theta_1)+p\phi_m) \cdot \sum_{n=p/2+1}^{\infty} J_n(m_{\mathrm{RF}})J_{n-p}(m_{\mathrm{RF}}) \cdot \sin\left((2n-p)\frac{\pi}{4}\right)\sin\left(\frac{\theta_2}{2}p(2n-p)\omega_{\mathrm{RF}}^2\right) \tag{18b}$$

for even harmonics of RF signal (p even) and

$$I_{p\mathrm{RF}}(p) = \pm 2\cos\left(p\frac{\pi}{4}\right)\sum_{n=(p+1)/2}^{\infty} S(n,p)J_n(m_{\mathrm{RF}})J_{n-p}(m_{\mathrm{RF}}) \cdot \cos\left(p\omega_{\mathrm{RF}}(t+\theta_1)+p\phi_m \pm S(n,p)\frac{\theta_2}{2}p(2n-p)\omega_{\mathrm{RF}}^2\right) \tag{18c}$$

for fundamental and odd harmonics of RF signal (p odd), where

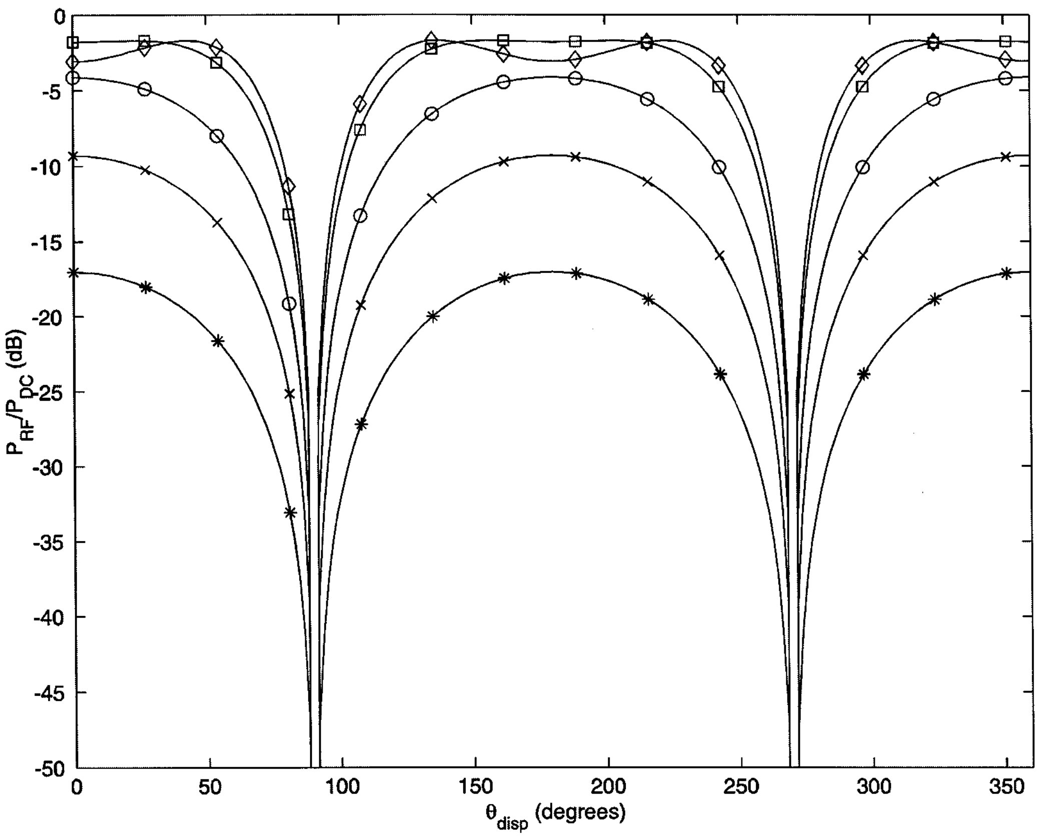

Fig. 4. Power of the detected signal RF component relative to dc detected power versus phase dispersion term $\theta_d = (\theta_2\omega_{\rm RF}^2)/2$ for different values of $m_{\rm RF}$ ($* = 0.1, x = 0.25, o = 0.5, \Box = 1, \Diamond = 1.25$) in the externally modulated analog dispersive optical link (DSB + C modulation) shown in Fig. 2.

$S(n, p)$ is a sign function expressed as

$$S(n, p) = \sin\left(n\frac{\pi}{2}\right) - (-1)^{(p-1)/2}\cos\left(n\frac{\pi}{2}\right) \tag{19}$$

and the sign uncertainty in (18a)–(18c) will define the upper (upper sign) or lower (lower sign) single-sideband optical modulation.

For example, we show the expression for the fundamental ($p = 1$) of the detected signal as

$$\begin{aligned} I_{p\rm RF}(1) =& \pm\sqrt{2}\sum_{n=1}^{\infty} S(n, 1)J_n(m_{\rm RF})J_{n-1}(m_{\rm RF}) \\ &\cdot\cos\left(\omega_{\rm RF}(t+\theta_1)+\phi_m \pm S(n, 1)\frac{\theta_2}{2}(2n-1)\omega_{\rm RF}^2\right) \\ =& \pm\sqrt{2}\left[J_1(m_{\rm RF})J_0(m_{\rm RF})\right. \\ &\cdot\cos\left(\omega_{RF}(t+\theta_1)+\phi_m \pm \frac{\theta_2}{2}\omega_{\rm RF}^2\right) \\ &+ J_2(m_{\rm RF})J_1(m_{\rm RF}) \\ &\left.\cdot\cos\left(\omega_{\rm RF}(t+\theta_1)+\phi_m \pm \frac{\theta_2}{2}3\omega_{\rm RF}^2\right)+\cdots\right]. \end{aligned} \tag{20}$$

From (20), it may be stated that the fundamental component is a sum of different terms, none of which suffers from dispersive attenuation. Furthermore, the optical link dispersion is translated to the electrical domain. For low modulation indexes, all the terms in eqn. (20) but the first term can be neglected obtaining the expected expression for a SSB + C optical modulation [10].

In Fig. 5, the amplitude and phase response of the RF component of the detected signal against dispersion phase term (θ_d) are plotted for five different values of optical modulation index, m_{RF}. As expected from eqn. (20), both amplitude and phase of detected signal are strongly dependent on optical modulation index when the optical link is dispersive. The ripples in the amplitude, phase and time delay at the different components of the detected signal [11] can be easily estimated from (18a)–(18c).

C. Harmonic Single-Sideband Up-Conversion (HSSB)

In order to generate an HSSB signal, the DD-MZM is driven in the same way as in SSB + C (Section IV-B), but a previous IF stage is included (Fig. 3). The general expressions presented in Section III are used to study the frequency component $I_{p\rm LO+IF}$ at the photodetector output. From (16e), it is possible to obtain the particular expression for the $I_{p\rm LO+IF}$ term as

$$\begin{aligned} &I_{p\rm LO+IF}(p) \\ &= \pm m_{\rm IF}\cos\left(p\frac{\pi}{4}\right)\cos\left(\frac{\theta_2}{2}\omega_{\rm IF}(p\omega_{\rm LO}+\omega_{\rm IF})\right) \\ &\cdot\sum_{n=(p+1)/2}^{\infty}\left[S(n, p)J_n(m_{\rm LO})J_{n-p}(m_{\rm LO})\right. \\ &\cdot\cos\left((p\omega_{\rm LO}+\omega_{\rm IF})(t+\theta_1)\right. \\ &+ p\phi_m + \phi_{\rm IFe} \pm S(n, p)\frac{\theta_2}{2}(2n-p) \\ &\left.\left.\cdot\,\omega_{\rm LO}(p\omega_{\rm LO}+\omega_{\rm IF})\right)\right] \end{aligned} \tag{21a}$$

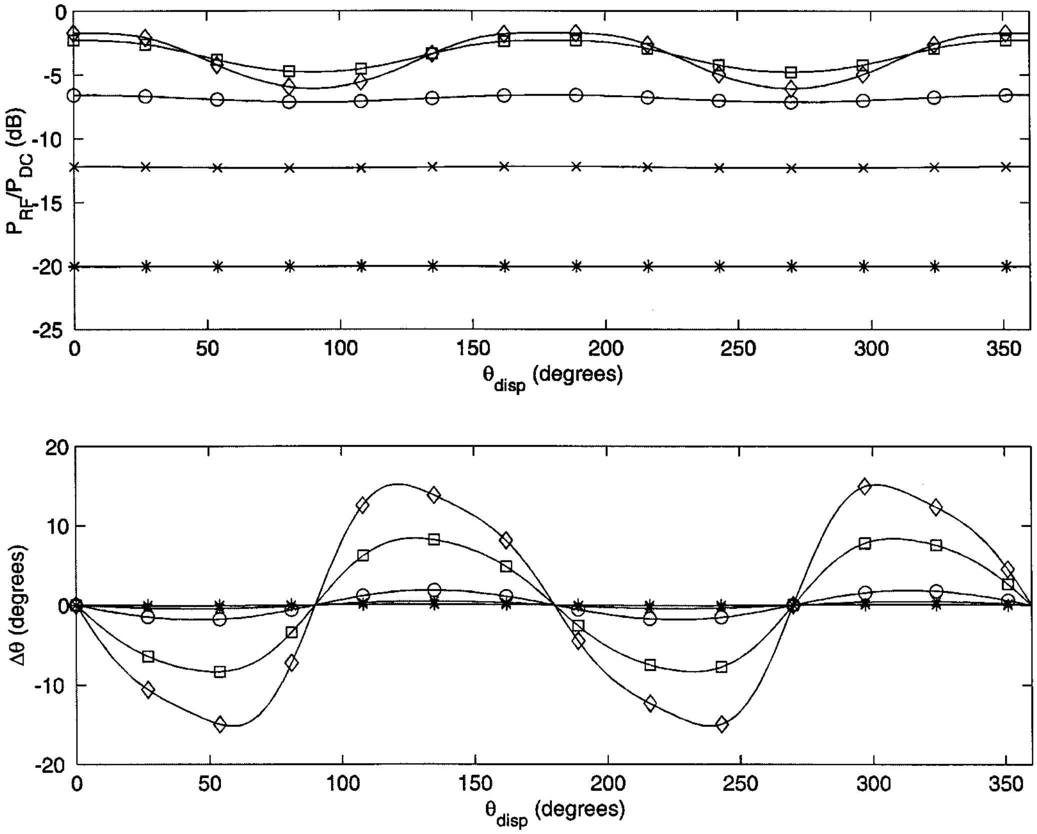

Fig. 5. Power of the detected signal RF component relative to dc detected power and detected phase ripple versus phase dispersion term $\theta_d = (\theta_2 \omega_{\mathrm{RF}}^2)/2$ for different values of m_{RF} ($* = 0.1, x = 0.25, o = 0.5, \square = 1, \diamond = 1.25$) in the externally modulated analog dispersive optical link (SSB + C modulation) from Fig. 2.

for p odd and

$$\begin{aligned} I_{p\mathrm{LO+IF}}(p) &= m_{\mathrm{IF}} \cos\left(\frac{\theta_2}{2}\,\omega_{\mathrm{IF}}(p\omega_{\mathrm{LO}}+\omega_{\mathrm{IF}})\right) \\ &\cdot \Bigg[\cos\left(p\frac{\pi}{4}\right)\cos\left((p\omega_{\mathrm{LO}}+\omega_{\mathrm{IF}})(t+\theta_1)+p\phi_m+\phi_{\mathrm{IFe}}\right) \\ &\cdot \Bigg[\frac{J_{p/2}^2(m_{\mathrm{LO}})}{2}(-1)^{p/2}+\sum_{n=p/2+1}^{\infty} J_n(m_{\mathrm{LO}})J_{n-p}(m_{\mathrm{LO}}) \\ &\cdot \cos\left(\frac{\theta_2}{2}(2n-p)\omega_{\mathrm{LO}}(p\omega_{\mathrm{LO}}+\omega_{\mathrm{IF}})\right)\Bigg] \\ &\mp \sin\left((p\omega_{\mathrm{LO}}+\omega_{\mathrm{IF}})(t+\theta_1)+p\phi_m+\phi_{IFe}\right) \\ &\cdot \sum_{n=p/2+1}^{\infty} J_n(m_{\mathrm{LO}})J_{n-p}(m_{\mathrm{LO}})\sin\left((2n-p)\frac{\pi}{4}\right) \\ &\cdot \sin\left(\frac{\theta_2}{2}(2n-p)\omega_{LO}(p\omega_{\mathrm{LO}}+\omega_{\mathrm{IF}})\right)\Bigg] \end{aligned} \tag{21b}$$

for p even, where $S(n,\, p)$ and the sign ambiguity are explained in Section IV-B.

Fig. 6 shows the amplitude of the RF term of the detected signal against RF frequency ($f_{\mathrm{RF}} = pf_{\mathrm{LO}}+f_{\mathrm{IF}}$) for second ($p = 2$) and third ($p = 3$) harmonics and for three different values of m_{LO} in an analog dispersive optical link [50 km of standard single-mode fiber with dispersion parameter $D = 17$ ps/(nm·km)] with a DD-MZM optical up-converter (HSSB with $m_{\mathrm{IF}} = 0.1$, $f_{\mathrm{IF}} = 500$ MHz). As expected from (21b) when $p = 2$, $I_{2\mathrm{LO+IF}}$ component vanishes when the dispersion is negligible but its level rapidly increases with frequency. On the contrary, $I_{3\mathrm{LO+IF}}$ term always exists but its level oscillates with frequency.

D. Harmonic Double-Sideband Up-Conversion (MITB/MATB/PSH)

The use of a standard MZM modulator, biased at the most nonlinear points, as an harmonic up-converter is a well known technique [2], [7]–[9]. If the MZM minimum transmission bias (MITB) point is selected, the optical carrier level at the MZM output is completely reduced. In this case, the MZM is biased at $|V_{\mathrm{DC1}} - V_{\mathrm{DC2}}| = V_\pi$ with a phase shift between MZM drives of $|\phi_{\mathrm{LO1}} - \phi_{\mathrm{LO2}}| = \pi$ [pseudo self-heterodyne modulation (PSH) from [9] is just a special case for MITB when we are only interested in the $I_{2\mathrm{LO}\pm\mathrm{IF}}$ term]. In the MITB case, the expressions for the dc or $I_{p\mathrm{LO+IF}}$ components at the photodetector output from (16) are reduced to

$$\begin{aligned} I_{\mathrm{DC}} &= \left[1+\frac{m_{\mathrm{IF}}^2}{8}\right]\sum_{n=-\infty}^{\infty} J_n^2(m_{\mathrm{LO}})\cos^2\left(\frac{\pi}{2}\pm n\frac{\pi}{2}\right) \\ &= 2\left[1+\frac{m_{\mathrm{IF}}^2}{8}\right]\sum_{k=0}^{\infty} J_{2k+1}^2(m_{\mathrm{LO}}) \end{aligned} \tag{22a}$$

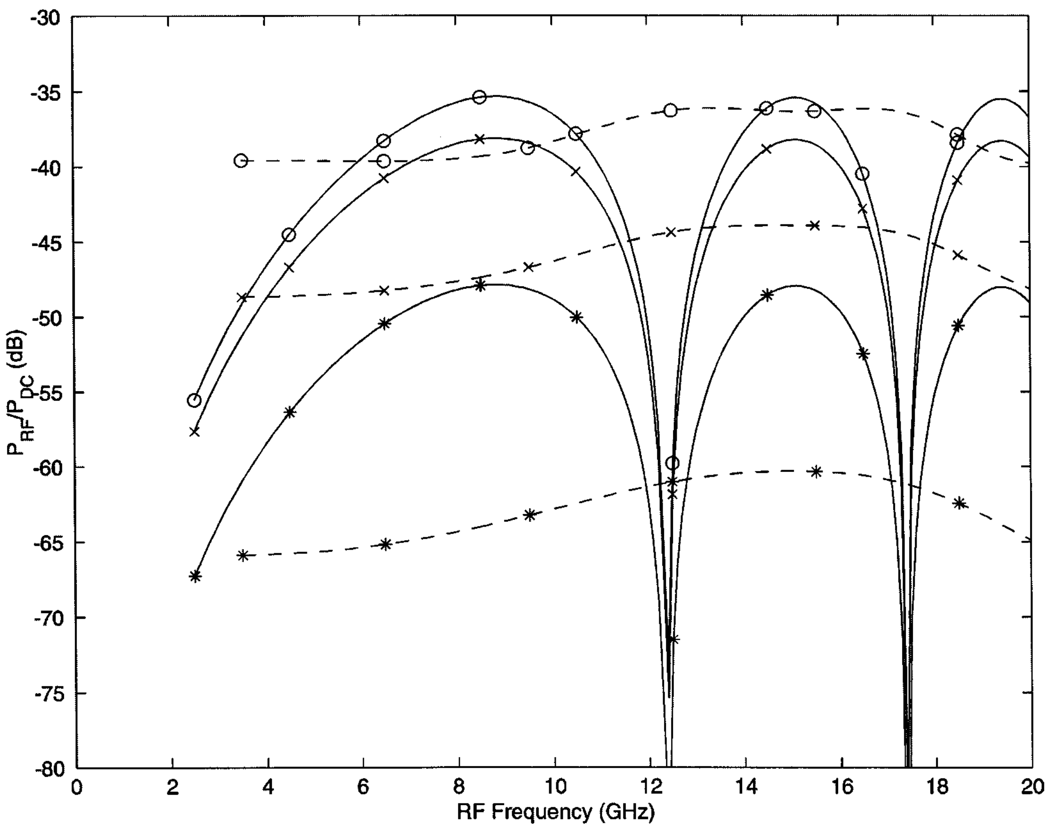

Fig. 6. Power of the detected signal RF component relative to dc detected power against RF frequency ($f_{\mathrm{RF}} = pf_{\mathrm{LO}} + f_{\mathrm{IF}}$) for second ($p = 2$, solid line) and third ($p = 3$, dashed line) harmonics and for three different values of m_{LO} ($* = 0.5, x = 1, o = 1.5$) in the analog dispersive optical link with a DD-MZM optical up-converter (HSSB with $m_{\mathrm{IF}} = 0.1$, $f_{\mathrm{IF}} = 500$ MHz) shown in Fig. 3.

$$\begin{aligned} I_{p\mathrm{LO+IF}}(p) &= m_{\mathrm{IF}} \cos\left(\frac{\theta_2}{2}\,\omega_{\mathrm{IF}}(p\omega_{\mathrm{LO}}+\omega_{\mathrm{IF}})\right) \\ &\quad\cdot \cos\left((p\omega_{\mathrm{LO}}+\omega_{\mathrm{IF}})(t+\theta_1)+p\phi_m+\phi_{\mathrm{IFe}}\right) \\ &\quad\cdot 2\sum_{k=p/4}^{\infty} J_{2k+1}(m_{\mathrm{LO}})J_{2k+1-p}(m_{\mathrm{LO}}) \\ &\quad\cdot \cos\left(\frac{\theta_2}{2}(4k+2-p)\omega_{\mathrm{LO}}(p\omega_{\mathrm{LO}}+\omega_{\mathrm{IF}})\right) \end{aligned} \tag{22b}$$

for p even and $p/2$ even, and

$$\begin{aligned} I_{p\mathrm{LO+IF}}(p) &= m_{\mathrm{IF}} \cos\left(\frac{\theta_2}{2}\,\omega_{\mathrm{IF}}(p\omega_{\mathrm{LO}}+\omega_{\mathrm{IF}})\right) \\ &\quad\cdot \cos\left((p\omega_{\mathrm{LO}}+\omega_{\mathrm{IF}})(t+\theta_1)+p\phi_m+\phi_{\mathrm{IFe}}\right) \\ &\quad\cdot \left[J_{p/2}^2(m_{\mathrm{LO}}) - 2\sum_{k=(p+2)/4}^{\infty} J_{2k+1}(m_{\mathrm{LO}})J_{2k+1-p}(m_{\mathrm{LO}}) \right.\\ &\quad\left.\cdot \cos\left(\frac{\theta_2}{2}(4k+2-p)\omega_{\mathrm{LO}}(p\omega_{\mathrm{LO}}+\omega_{\mathrm{IF}})\right)\right] \end{aligned} \tag{22c}$$

for p even and $p/2$ odd. When MITB is selected, all $I_{p\mathrm{LO+IF}}$ terms are zero for p odd.

If the maximum transmission bias point is selected instead of the MITB point, the optical carrier level at the MZM output is completely maximized. In this case, the MZM is biased at $|V_{\mathrm{DC1}} - V_{\mathrm{DC2}}| = 0$ with a phase shift between MZM drives of $|\phi_{\mathrm{LO1}} - \phi_{\mathrm{LO2}}| = \pi$. In the MATB case, the following expression is particularized from (16):

$$\begin{aligned} I_{\mathrm{DC}} &= \left[1+\frac{m_{\mathrm{IF}}^2}{8}\right]\sum_{n=-\infty}^{\infty} J_n^2(m_{\mathrm{LO}})\cos^2\left(n\frac{\pi}{2}\right) \\ &= \left[1+\frac{m_{\mathrm{IF}}^2}{8}\right]\left[J_0^2(m_{\mathrm{LO}}) + 2\sum_{k=0}^{\infty} J_{2k}^2(m_{\mathrm{LO}})\right] \end{aligned} \tag{23a}$$

$$\begin{aligned} I_{p\mathrm{LO+IF}}(p) &= m_{\mathrm{IF}} \cos\left(\frac{\theta_2}{2}\,\omega_{\mathrm{IF}}(p\omega_{\mathrm{LO}}+\omega_{\mathrm{IF}})\right) \\ &\quad\cdot \cos\left((p\omega_{\mathrm{LO}}+\omega_{\mathrm{IF}})(t+\theta_1)+p\phi_m+\phi_{\mathrm{IFe}}\right) \\ &\quad\cdot \left[J_{p/2}^2(m_{\mathrm{LO}}) + 2\sum_{k=p/4+1}^{\infty} J_{2k}(m_{\mathrm{LO}})J_{2k-p}(m_{\mathrm{LO}}) \right.\\ &\quad\left.\cdot \cos\left(\frac{\theta_2}{2}(4k-p)\omega_{\mathrm{LO}}(p\omega_{\mathrm{LO}}+\omega_{\mathrm{IF}})\right)\right] \end{aligned} \tag{23b}$$

for p even and $p/2$ even, and

$$I_{p\mathrm{LO+IF}}(p) = -m_{\mathrm{IF}} \cos\left(\frac{\theta_2}{2}\,\omega_{\mathrm{IF}}(p\omega_{\mathrm{LO}}+\omega_{\mathrm{IF}})\right) \cdot \cos\left((p\omega_{\mathrm{LO}}+\omega_{\mathrm{IF}})(t+\theta_1)+p\phi_m+\phi_{\mathrm{IFe}}\right) \cdot 2\sum_{k=(p+2)/4}^{\infty} J_{2k}(m_{\mathrm{LO}})J_{2k-p}(m_{\mathrm{LO}}) \cdot \cos\left(\frac{\theta_2}{2}\,(4k-p)\omega_{\mathrm{LO}}(p\omega_{\mathrm{LO}}+\omega_{\mathrm{IF}})\right) \quad (23c)$$

for p even and $p/2$ odd. As it happened with MITB, when MATB is selected, all $I_{p\mathrm{LO+IF}}$ terms are zero for p odd.

From the particular expressions in (22a)–(22c) and (23a)–(23c), understanding and assessing the dispersive attenuation and gain ripple shown by the optical up-conversion schemes based on DD-MZM biased on MITB/MATB is straightforward [8], [11].

V. Verification of Analysis

In order to assess the validity of the expressions shown here, several time-domain simulations were carried out with the commercial program OptSim 3.1 from ARTIS Software Corporation. The result of these simulations was a complete agreement between this paper expressions and the OPTSIM simulation of the configurations shown in Figs. 2 and 3. As an example of this agreement, the position of the different symbols ($*$, $\times$, o, $\square$, $\diamondsuit$) in Figs. 4–6 correspond to OPTSIM results while the corresponding solid/dashed lines were extracted from the expressions in this paper.

VI. Conclusion

The general and rigorous expressions for an IM/DD dispersive analog link with a DD-MZM modulator or up-converter have been presented and demonstrated. With these general expressions, it is straightforward to study the amplitude, phase, or time delay suffered by the desired frequency component (fundamental or harmonic) of the detected signal.

All the usual analog modulation formats (DSB + C, SSB + C) and up-conversion schemes (HSSB, MITB, MATB, PSH) based on standard MZM or DD-MZM can be particularized from the general expressions. The dispersive link could refer to any length of standard single-mode fiber, highly dispersive fiber, or linearly chirped fiber gratings.

When the DD-MZM is used as an optical modulator (DSB + C, SSB + C), the performance for any modulation against fiber chromatic dispersion can be analyzed without any restriction on RF level. Also, nonlinear behavior (detected signal compression or harmonic content) for these modulations can be studied. When the DD-MZM is used as an optical up-converter (HSSB, MITB, MATB, PSH), the selection of the optimum LO level can be addressed just by analyzing the complete expression for the harmonic of interest taking into account the influence of optical link chromatic dispersion. Different harmonic up-conversion configurations can be easily studied in terms of dispersive attenuation, dynamic range or amplitude and phase ripple.

Finally, the general expressions for analog IM/DD dispersive links with a DD-MZM presented here allow the study of new modulation or up-conversion schemes.

References

[1] S. Komaki, K. Tsukamoto, and M. Okada, "Requirements for radio-wave photonic devices from the viewpoint of future mobile radio systems," *IEEE Trans. Microwave Theory Tech.*, vol. 43, pp. 2222–2228, Sept. 1995.

[2] R. Hofstetter, H. Schmuck, and R. Heidemann, "Dispersion effects in optical mm-wave systems using self-heterodyne method for transport and generation," *IEEE Trans. Microwave Theory Tech.*, vol. 43, pp. 2263–2269, Sept. 1995.

[3] H. Schmuck, "Comparison of optical mm-wave system concepts with regard to chromatic dispersion," *Electron. Lett.*, vol. 31, pp. 1848–1849, Oct. 1995.

[4] R. D. Esman, M. J. Monsma, J. L. Dexter, and D. G. Cooper, "Microwave true time-delay modulator using fiber-optic dispersion," *Electron. Lett.*, vol. 28, pp. 1905–1907, Sep. 1992.

[5] J. L. Corral, J. Marti, J. M. Fuster, and R. I. Laming, "Dispersion-induced bandwidth limitation of variable true time delay lines based on linearly chirped fiber gratings," *Electron. Lett.*, vol. 34, pp. 209–211, Jan. 1998.

[6] G. H. Smith, D. Novak, and Z. Ahmed, "Novel technique for generation of optical SSB with carrier using a single MZM to overcome fiber chromatic dispersion," in *Int. Microwave Photon. Topical Meeting*, Dec. 1996, Paper PDP-2.

[7] G. P. Gopalakrishnan, W. K. Burns, and C. H. Bulmer, "Microwave-optical mixing in $LiNbO_3$ modulators," *IEEE Trans. Microwave Theory Tech.*, vol. 41, pp. 2383–2391, Dec. 1993.

[8] J. M. Fuster, J. Marti, J. L. Corral, V. Polo, and F. Ramos, "Generalized study of dispersion-induced power penalty mitigation techniques in millimeter-wave fiber-optic links," *J. Lightwave Technol.*, vol. 18, pp. 933–940, July 2000.

[9] J. L. Corral, J. Marti, and J. M. Fuster, "Optical up-conversion on continuously variable true time delay lines based on chirped fiber gratings for millimeter-wave optical beamforming networks," *IEEE Trans. Microwave Theory Tech.*, vol. 47, pp. 1315–1320, July 1999.

[10] G. H. Smith, D. Novak, C. Lim, and K. Wu, "Full-duplex broadband millimeter-wave optical transport system for fiber-wireless access," *Electron. Lett.*, vol. 33, pp. 1159–1160, June 1997.

[11] J. L. Corral, J. Marti, and J. M. Fuster, "Effects of optical modulation on continuously variable millimeter-wave delay lines based on optical fiber gratings," in *IEEE MTT-S Int. Microwave Symp. Dig.*, Anaheim, CA, June 1999, pp. 1117–1120.

Juan L. Corral (S'90–A'98–M'01) was born in Zaragoza, Spain, on April 20, 1969. He received the Ingeniero de Telecomunicación degree (with first-class honors) and the Doctor Ingeniero de Telecomunicación degree from the Universidad Politécnica de Valencia, Valencia, Spain, in 1993 and 1998, respectively.

During 1993, he was an Assistant Lecturer in the Departamento de Comunicaciones, Universidad Politécnica de Valencia. From 1993 to 1995, he was with the Microwave Technology and Equipment Section (XRM), European Space Research and Technology Centre (ESTEC), European Space Agency (ESA), Noordwijk, The Netherlands, where he was engaged in research on MMIC-based technologies and photonics technologies for beamforming networks for on-board phased-array antennas. In 1995, he joined the Communications Departament, Universidad Politécnica de Valencia, where he became an Associate Professor in 2000. His research interests include phased-array antennas, optical beamforming networks, digital beamforming and microwave and millimeter-wave optical-fiber systems. He has authored or co-authored over 30 papers in international journal and conference proceedings in his areas of research interests.

Dr. Corral is a member of several IEEE societies. He was the recipient of the 1998 Doctorate Prize of the Telecommunications Engineer Association in Spain for his Ph.D. dissertation on applications of MMIC and photonic technologies to phased-array antennas.

Javier Marti (S'89–M'92) received the Ingeniero de Telecomunicación degree from the Universidad Politecnica de Catalunya, Catalunya, Spain, in 1991, and the Doctor Ingeniero de Telecomunicacion degree (Ph.D.) from the Universidad Politecnica de Valencia, Valencia, Spain, in 1994.

During 1989 and 1990, he was an Assistant Lecturer at the Escuela Universitaria de Vilanova, Barcelona, Spain. From 1991 to 2000, he was a Lecturer and Associate Professor at the Telecommunication Engineering Faculty, where he is currently a Professor and leads the Radio over Fiber Group. He has authored or co-authored over 90 papers in refereed international technical journals and over 40 papers in international conference proceedings in the fields of fiber-radio and microwave/millimeter-wave photonics, wavelength division multiplexing (WDM) and SCM optical networks systems, optical processing of microwave signals, and dispersion and fiber nonlinearities compensation employing fiber gratings and other techniques.

Dr. Marti is member of the Technical Program Committee of ECOC and several other international workshops and conferences.

Jose M. Fuster was born in Tarragona, Spain, on March 23, 1970. He received the M.Sc. and Ph.D. degrees in telecommuincations engineering from the Universidad Politécnica de Valencia, Valencia, Spain, in 1993 and 1998, respectively.

Since 1993, he has been a Lecturer in the Departamento de Comunicaciones, Universidad Politécnica de Valencia, where he is member of the Radio over Fiber Group. In 1999, he was with the Photonics Research Laboratory, University of Melbourne, Melbourne, Australia, during a research stage of three months. In November 1999, he become an Associate Professor at the Universidad Politécnica de Valencia. His research interests include microwave and millimeter-wave optical-fiber links, phased-array antennas, electrooptic modulators, and optical networks.